Food and Chemical Toxicology 121 (2018) 115–123

Contents lists available at ScienceDirect

Food and Chemical Toxicology

journal homepage: www.elsevier.com/locate/foodchemtox

Application of the comparison approach to open TG-GATEs: A useful toxicogenomics tool for detecting modes of action in chemical risk assessment

Harm J. Heusinkveld[a,b,*], Paul F.K. Wackers[a], Willem G. Schoonen[c], Leo van der Ven[a], Jeroen L.A. Pennings[a], Mirjam Luijten[a]

[a] Centre for Health Protection, National Institute for Public Health and the Environment (RIVM), Bilthoven, The Netherlands
[b] Neurotoxicology Research Group, Toxicology and Pharmacology Division, Institute for Risk Assessment Sciences (IRAS), Utrecht University, Utrecht, The Netherlands
[c] Centre for Nutrition, Prevention and Health Services, National Institute for Public Health and the Environment (RIVM), Bilthoven, The Netherlands

ARTICLE INFO

Keywords:
In vitro
Gene expression
Human health risk assessment
Liver
Pharmaceuticals
Transcriptomics

ABSTRACT

Mode of action information is one of the key components for chemical risk assessment as mechanistic insight leads to better understanding of potential adverse health effects of a chemical. This insight greatly facilitates assessment of human relevance and enhances the use of non-animal methods for risk assessment, as it ultimately enables extrapolation from initiating events to adverse effects. Recently, we reported an in vitro toxicogenomics comparison approach to categorize (non-)genotoxic carcinogens according to similarities in their proposed modes of action. The present study aimed to make this comparison approach generally applicable, allowing comparison of outcomes across different studies. The resulting further developed comparison approach was evaluated through application to toxicogenomics data on 18 liver toxicants in human and rat primary hepatocytes from the Open TG-GATEs database. The results showed sensible matches between compounds with (partial) overlap in mode of action, whilst matches for compounds with different modes of action were absent. Comparison of the results across species revealed pronounced and relevant differences between primary rat and human hepatocytes, underpinning that information on mode of action enhances assessment of human relevance. Thus, we demonstrate that the comparison approach now is generally applicable, facilitating its use as tool in mechanism-based risk assessment.

1. Introduction

Insight into the mode of action (MOA) of a chemical leads to better understanding of its potential adverse health effects, thereby facilitating assessment of the relevance of effects to humans. In addition, MOA information greatly enhances the use of non-animal methods for risk assessment, as it will ultimately enable extrapolation from initiating events to adverse effects. Acceptation and implementation of approaches that predict adverse health effects based on earlier key events will be strongly facilitated through the implementation of a framework for organizing mechanistic information in a consistent and transparent manner. Both the MOA/human relevance concept (Meek et al. 2003, 2014; Sonich-Mullin et al., 2001) and the Adverse Outcome Pathway (AOP) concept (Ankley et al., 2010) offer such a framework.

A chemical class for which a mechanism-based risk assessment process would be especially useful is the class of non-genotoxic carcinogens (NGTXCs). NGTXCs act through secondary mechanisms that do not involve direct interaction with DNA. Instead, these compounds act through a large and diverse variety of well-known mechanisms including immune suppression, and inflammatory responses (Hanahan and Weinberg 2000, 2011; Hernandez et al., 2009; Jacobs et al., 2016; Williams, 2001). Recently, we presented an in vitro toxicogenomics comparison approach to categorize (non-)genotoxic carcinogens according to similarities in their proposed MOA(s) (Schaap et al. 2012, 2015). This comparison approach addresses the need to obtain detailed knowledge about the MOA(s) of a chemical of interest and its concept is universally applicable to environmental and pharmaceutical chemicals.

The aim of the present study was to make the comparison approach generally applicable allowing comparison of outcomes across different studies. This will facilitate its use as a tool in chemical risk assessment. For this, we used data from the publicly available Toxicogenomics

* Corresponding author. Centre for Health Protection, P.O. Box 1, 3720 BA, Bilthoven, The Netherlands.
E-mail address: Harm.Heusinkveld@rivm.nl (H.J. Heusinkveld).

https://doi.org/10.1016/j.fct.2018.08.007
Received 13 June 2018; Received in revised form 20 July 2018; Accepted 5 August 2018
Available online 08 August 2018
0278-6915/

Project-Genomics Assisted Toxicity Evaluation System database (Open TG-GATEs; http://toxico.nibiohn.go.jp/english (Igarashi et al., 2015)). The Open TG-GATEs database comprises toxicogenomics data for a large number of different substances (170), generated with in vitro studies using human and rat primary hepatocytes as well as in vivo studies in rat. In addition, the availability of data from several time points and dosages as well as the inclusion of three biological replicates rendered Open TG-GATEs the database of choice. Using this database, we were able to improve several aspects of the comparison approach while leaving its concept unchanged. We evaluated the further developed approach through application to a selected set of substances that are all known to affect the liver, covering several modes of action and pathological outcomes. We focused on data obtained from human and rat primary hepatocytes. By comparing the results for substances with similar and different MOAs, also across species, we demonstrate the applicability and the usefulness of the comparison approach as a tool in mechanism-based risk assessment.

2. Materials and methods

2.1. Compound selection

For the study presented here, a subset of 18 compounds was selected from the Open TG-GATEs database. Details including dosages used are given in Table 1. This subset was assembled by including known human and rodent hepato-carcinogens as well as non-carcinogenic hepatotoxicants with varying primary MOAs and (in vivo) pathological outcomes. This dataset consisted of three concentrations (low, mid, high) for all compounds in both in vitro models, except for ETH, ETP, FFB and IBU where data from primary human hepatocytes for the low concentration was missing. Information on possible toxic MOAs in human and rodent liver has been collected through literature searches using the PubMed database and, where applicable, the AOPWiki (http://www.aopkb.org).

2.2. General data analysis

Raw data for compound exposures and corresponding controls were downloaded as CEL files from Open TG-GATEs (http://toxico.nibiohn.go.jp/english; (Igarashi et al., 2015)). Normalized expression values were calculated using the robust multi-chip average (RMA) algorithm (Affy package, version 1.48.0) (Irizarry et al., 2003) using the standard Affymetrix probe set information for the Rat Genome 230 2.0 Array (for rat primary hepatocyte data) and the Human Genome U133 Plus 2.0 Array (for human primary hepatocyte data). To remove gene redundancy, probe sets were collapsed to their corresponding Entrez gene ID provided in the rat2302. db (rat, version 3.3.2) and hgu133plus2. db (human, version 3.2.2) R packages, respectively (Carlson et al., 2016). This resulted in a table with 14,416 genes for rat and 20,546 genes for human. Subsequent to normalization, using density plots, boxplots, and principal component analysis, the data was visualized as a check for statistical testing. Differential gene expression between the experimental groups and the control group were determined using the Limma package (version 3.26.9; (Phipson et al., 2016)) in R statistical software version 3.3.1 (http://cran.r-project.org). Per compound and per concentration, the top 1000 most significantly regulated genes (according to their absolute T-statistic, referred as |T|) were mapped against the Kyoto Encyclopedia of Genes and Genomes (KEGG) database (http://www.kegg.jp/) using the KEGGREST package (version 1.10.1; http://bioconductor.org/packages/KEGGREST/). Overlapping genes were identified according to their ENTREZ gene ID. P-values were calculated using a hypergeometric test.

3. Results

3.1. Method development

The starting point for this study was the comparison approach as previously described (Schaap et al., 2015). In short, this method starts with selecting the 50 (n in following formulas) most differentially expressed genes based on their T-statistics, ranking the resulting gene sets followed by determining mutual overlap between compound exposures, and combining the T-statistics for these genes into a score per gene, which are then combined into an overall score. For an overview of this approach please see the publication by Schaap and co-workers (Schaap et al., 2015).

For the further development of the comparison approach (see below) we explored various scoring methods. First, to make the comparison approach general applicable and to respect the gene expression proportions, we tested re-scaling the |T| to a value within a predefined range, yet that is based on the distribution of |T|, which led to the re-scaled score S for gene i being calculated as:

$$S_i = \frac{|T|_i - |T|_{min}}{|T|_{max} - |T|_{min}} * n$$

This turned out to introduce artefacts. For example, a compound with low and relatively constant |T| values may get higher scores than a compound where the top |T| values are high, followed by a rapid decline in |T|. Moreover, |T| scores are to some extent dependent on the experimental setup, e.g. the number of replicates used. To ensure general applicability of our method, we opted for using reverse rank-based gene scores (i.e. $S_i = n - (i - 1)$) as indicated in Fig. 1.

Another question that arose in relation to calculating rank-based gene scores was whether this should be done per compound or over compounds, i.e. by jointly comparing data for two compounds. Assigning scores by ranking the |T| within each compound in a comparison appeared more straightforward and thus better suited for a generally applicable approach as the ranking could be automated for each compound separately. However, when ranking the |T| per compound, the 50 highest ranking |T| values for a compound with low value |T| get weighed as important as the 50 highest |T| for a compound with high |T| (see example in Supplemental Figure 1). This especially creates artefacts for compound comparisons where the magnitude of the top 50 responses is considerably different. The need to avoid such artefacts in compound comparisons led us to the method of linear ranking |T| values over the two compounds in a comparison.

For combining these (reverse) rank-based scores into a score per gene, we explored two methods that are sufficiently generically applicable, namely summation as well as multiplication of the two reverse rank scores. From a mathematical point of view, multiplication would yield larger scores if the overlap among hits would extend to those with the higher gene scores, thus potentially creating additional accuracy and resolution for our method. On the other hand, genes for which one of the reverse rank scores are zero would get an overall zero score with a multiplication, thus erasing possible subtle effects. Upon evaluation, we observed that for different doses of a compound summation of gene scores resulted in a slightly higher resolution than multiplication.

Finally, we tested the use of different numbers of top-ranking |T| values as input for the comparison approach, by comparing a top 30, 50, 75 and 100. For less than 50 genes, the sensitivity for detecting the same MOA across multiple doses of a compound was poor; using over 100 genes appeared to reduce the specificity as several compounds with dissimilar MOAs showed overlap in their top-ranking genes (data not shown). Therefore, we opted for using the top 50 genes.

3.2. Flowchart with method description

The workflow of the resulting refined comparison approach depicted in Fig. 1 is described here in more detail, using data for

Table 1
Selected compounds from the Open TG-GATEs database.

Compound	Abbreviations	CAS RN	Pharmaceutical classification	Dose R (uM)	Dose H (uM)	MOA	References
Acetaminophen	APAP	103-90-2	Analgesic	1000 3000 10000	200 1000 5000	Formation of toxic metabolite leading to glutathione depletion, oxidative stress and mitochondrial dysfunction leading to ATP depletion leading to liver necrosis	(Yoon et al., 2016)
Amiodarone	AM	1951-25-3	Antiarrhythmic	0.28 1.40 7.00	0.28 1.40 7.00	Inhibition of mitochondrial fatty acid (FA) oxidation leading to imbalance between FA uptake, de novo lipogenesis, FA oxidation, and lipid efflux leading to increased hepatic FA and triglyceride levels leading to phospholipidosis and steatosis	(Angrish et al., 2016; Begriche et al., 2011; van de Water et al., 2011)
Azathioprine	AZP	446-86-6	Immunosuppressant	0.14 0.72 3.60	2.9 14.6 72.8	Degradation of 6-thioguanine metabolites via xanthine oxidase leading to reactive oxygen species (ROS)-induced DNA damage and mitochondrial dysfunction leading to cell cycle arrest and apoptosis	(Karran, 2006; Tapner et al., 2004)
Carbamazepine	CBZ	298-46-4	Antiepileptic	12 60 300	12 60 300	Sustained endoplasmic reticulum (ER) stress, activation of the unfolded protein response and Nrf2-mediated oxidative stress response leading to hepatic necrosis	(Fredriksson et al., 2014; Iida et al., 2015; Malhi and Kaufman, 2011)
Chlorpromazine	CPZ	50-53-3	Antipsychotic	0.8 4 20	0.8 4 20	Accumulation of bile acids leading to oxidative stress, inflammation, and activation of nuclear receptors leading to cholestasis	(Antherieu et al., 2013; Selim and Kaplowitz, 1999; van de Water et al., 2011; Vinken et al., 2013; Yang et al., 2013)
Clofibrate	CFB	637-07-0	Antilipidemic	12 60 300	12 60 300	Sustained PPARalpha signaling leading to perturbation of cell growth and survival leading to liver tumors	(Corton et al., 2014)
Cyclophosphamide	CPA	50-18-0	Chemotherapeutic	8 40 200	80 400 2000	Formation of DNA strand breaks leading to cell cycle arrest and apoptosis; Formation of toxic metabolite leading to Nrf2-mediated oxidative stress response leading to hepatic necrosis	(DeLeve, 1996; Elshater et al., 2017; Kawabata et al., 1990; Murata et al., 2004)
Cyclosporine A	CSA	59865-13-3	Immunosuppressant	0.24 1.2 6	0.24 1.2 6	Accumulation of bile acids leading to oxidative stress, inflammation, and activation of nuclear receptors, leading to cholestasis; Sustained ER stress leading to activation of the unfolded protein response and mitochondrial dysfunction leading to cell death	(Antherieu et al., 2013; Foufelle and Fromenty, 2016; Korolczuk et al., 2016; Selim and Kaplowitz, 1999; Szalowska et al., 2013; van de Water et al., 2011; Vinken et al., 2013; Yang et al., 2013)
Diclofenac	DFNa	15307-86-5	Nonsteroidal anti-inflammatory	16 80 400	16 80 400	Formation of toxic metabolite leading to ER stress, activation of the unfolded protein response and Nrf2-mediated oxidative stress response leading to cell death; PPARγ activation leading to mitochondrial dysfunction, oxidative stress and inflammation leading to liver necrosis	(Bessone, 2010; Fredriksson et al., 2014; Malhi and Kaufman, 2011; Nouri et al., 2017; Puhl et al., 2015)
Ethionamide	ETH	536-33-4	Anti-tuberculosis	24 120 600	120 600	Formation of toxic metabolite leading to oxidative stress and inflammation leading to hepatotoxicity; Sustained ER stress leading to apoptosis	(Henderson et al., 2008; Ramappa and Aithal, 2013; Reyes-Gordillo et al., 2017; Sutherland et al., 2017)
Etoposide	ETP	33419-42-0	Chemotherapeutic	14 70 350	66 330	Topoisomerase II poison leading to DNA double-strand breaks leading to apoptosis; Formation of ROS leading to oxidative stress, inflammation, and activation of nuclear receptors, leading to cholestasis	(Choudhury et al., 2004; Grigorian and O'Brien, 2014)
Fenofibrate	FFB	49562-28-9	Antilipidemic	1.2 6 30	6 30	Sustained PPARα signalling leading to perturbation of cell growth and survival leading to liver tumors in rodents	(Corton et al., 2014)
Ibuprofen	IBU	15687-27-1	Nonsteroidal anti-inflammatory	40 200 1000	30 150	PPARγ activation leading to mitochondrial dysfunction, oxidative stress and inflammation leading to liver necrosis	(Bessone, 2010; Puhl et al., 2015)
Perhexeline	PH	6621-47-4	Antianginal	0.4 2 10	0.6 3 15	Inhibition of oxidative phosphorylation and mitochondrial FA oxidation leading to imbalance between FA uptake, de novo lipogenesis, FA oxidation, and lipid efflux leading to increased hepatic FA and triglyceride levels leading to steatosis and steatohepatitis	(Begriche et al., 2011)

(*continued on next page*)

Table 1 (*continued*)

Compound	Abbreviations	CAS RN	Pharmaceutical classification	Dose R (uM)	Dose H (uM)	MOA	References
Rifampicin	RIF	13292-46-1	Anti-tuberculosis	2.8 14 70	2.8 14 70	PXR activation leading to sustained activation of CYP and phase II enzymes, induction of oxidative stress response and lipid peroxidation leading to steatohepatitis; Altered activity of hepatocyte transporters leading to interference with canalicular excretion of bile salts leading to cholestasis	(Kullak-Ublick and Becker, 2003; Ramappa and Aithal, 2013; Staudinger et al., 2013)
Tunicamycin	TUN	11089-65-9	Antibiotic	2 10 50	0.4 2 10	Sustained ER stress leading to activation of the unfolded protein response leading to apoptosis; Sustained ER stress leading to imbalance between FA uptake, de novo lipogenesis, FA oxidation, and lipid efflux leading to increased hepatic FA and triglyceride levels leading to steatosis	(Foufelle and Fromenty, 2016; Malhi and Kaufman, 2011)
Valproic Acid	VPA	99-66-1	Antiepileptic	400 2000 10000	200 1000 5000	Inhibition of mitochondrial FA oxidation leading to imbalance between FA uptake, de novo lipogenesis, FA oxidation, and lipid efflux leading to increased hepatic FA and triglyceride levels leading to steatosis	(Angrish et al., 2016; Begriche et al., 2011; Lampen et al., 2001)
WY-14,643	WY	50892-23-4	Antilipidemic	8 40 200	6 30 150	Sustained PPARα signalling leading to perturbation of cell growth and survival leading to liver tumors in rodents	(Corton et al., 2014)

rifampicin (RIF, medium dose) and cyclophosphamide (CPA, high dose) as an example. Data supporting this example are given in supplemental file 1. As a first step, differentially expressed genes are ranked according to their |T|. Per compound, the 50 genes with the highest |T| are selected for the analysis (A, Fig. 1; Supplemental file 1, Table B). In step B, the selected genes are ranked according to their |T| over both compounds. A score from 50 to 1 is assigned to the 50 genes with the highest |T| (B, Fig. 1; Supplemental file 1, Table B). Subsequently, the intersection of genes is determined. Only overlapping genes regulated in the same direction are taken into account for analysis (C, Fig. 1; Supplemental file 1, Table B, green and red coloured ENTREZ gene IDs). Non-overlapping genes or overlapping genes with opposite regulation are omitted (D, Fig. 1; Supplemental file 1, Table B, grey coloured ENTREZ gene IDs). For the overlapping genes (further referred to as 'hits'), the assigned scores for both compounds are summed, resulting in a total score per hit (Supplemental file 1, Table E). These scores are summed for all hits, resulting in a match score per compound comparison (E, Fig. 1; Supplemental file 1, Table E). In case data for multiple concentrations or doses per compound are available, multiple match scores are calculated. In the final step the maximum score across doses/concentrations is determined (F, yellow marked cell, Fig. 1; Supplemental file 1, Table F).

3.3. Application of methodology

Next, the further developed approach was evaluated through application to the toxicogenomics data obtained in human and rat primary hepatocytes following 24 h exposure to the selected compounds listed in Table 1. The resulting scores are displayed in Table 2A for primary rat hepatocytes and in Table 2B for primary human hepatocytes. A match between compounds was considered relevant when the number of hits (directionally overlapping genes) out of the top 50 (C in Fig. 1) and the maximum score value across concentrations was larger than 10 and 500, respectively (E in Fig. 1; Table 2A and 2B, matches marked green). A match was considered weak but potentially relevant when the number of hits was larger than 10 but the maximum score across concentrations did not reach 500 (Table 2A and 2B, matches marked yellow). Among the 18 compounds, amiodarone (AM) did not display a relevant match according to the cut-off values set, neither for human nor for rat. This is probably due to a very weak gene expression response for all concentrations of AM tested, which is reflected by the absence of differentially expressed genes for both rat and human hepatocytes (data not shown). Nevertheless, pathway analysis based on the top 1000 regulated genes according to T-statistics revealed a (low) number of significantly enriched relevant pathways ($p < 0.001$; Supplemental file 3) in the primary rat hepatocytes but not in the human primary hepatocytes (Supplemental file 4). However, these pathways, involved in steroid biosynthesis and fatty acid metabolism/degradation, were only observed for the highest concentration tested (7 μM) indicating that the concentration range used in this study (i.e. 0.28–7 μM) was probably too low to induce an effect. This is in line with literature data where the most sensitive effect (phospholipidosis) in vitro has been reported from 3 μM onwards (see e.g. (van de Water et al., 2011)).

For the primary rat hepatocytes (Table 2A), the major findings consisted of a consistent match between the PPARalpha agonists WY, FFB and CFB with the NSAIDs DFNa and IBU as well as with VPA (Table 2A). Additionally, the comparison approach yielded matches between PH, AZP and CPZ, as well as between RIF, ETP, CSA and IBU. The compounds APAP, CBZ, ETH and TUN did not have a relevant match with any of the 18 compounds studied.

Analogous to the results for rat cells, we observed for primary human hepatocytes a clear match between the PPARalpha agonists (WY, FFB, CFB) and the NSAIDs (DFNa and IBU) (Table 2B). However, the additional match with VPA observed in rat cells, was missing in human cells. Other relevant matches observed were between WY, CPA and RIF as well as between ETP, CSA, DFNa and TUN. VPA and ETH

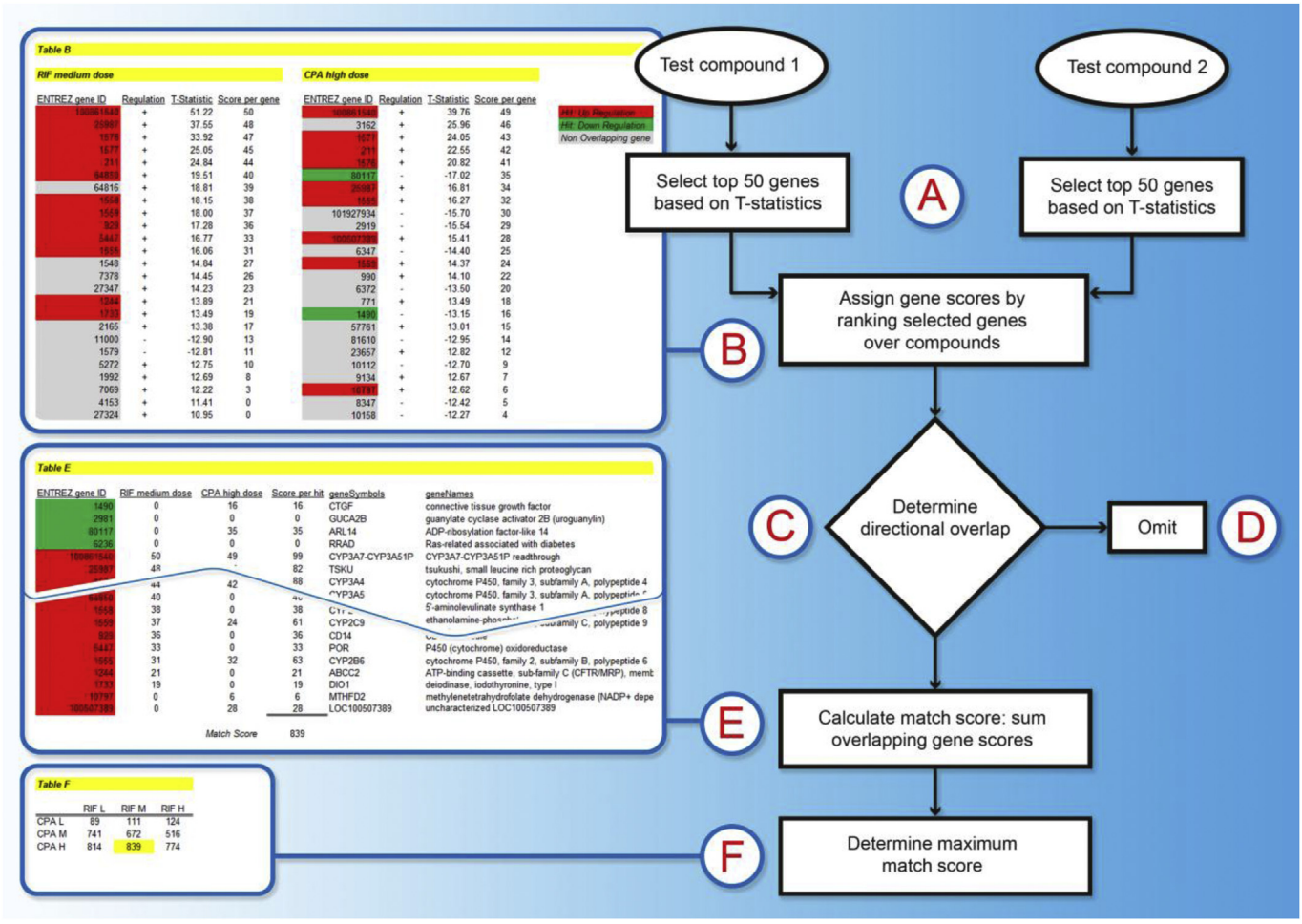

Fig. 1. Flowchart of workflow for the new generic applicable, further developed comparison approach. For explanation of the labels A – F, see paragraph 3.2.

gave only weak matches (see Table 2B), all of which were absent in rat.

4. Discussion

We developed an improved version of the previously reported comparison approach and tested its generic applicability through application to data from the Open TG-GATEs database. All 18 compounds used for the evaluation were selected based on their potential to induce hepatotoxicity with a range of, partially overlapping, MOAs. Pathway analyses were conducted to aid interpretation (Supplemental files 3 and 4). These analyses revealed the virtual absence of significantly regulated pathways for AM, for which also no convincing match was observed. For other compounds without a convincing match, e.g. ethionamide (ETH), many strongly regulated pathways were identified, which illustrated absence of overlap in MOA with the other compounds. MOAs detected include DNA damage, p53-mediated pathways, endoplasmic reticulum stress, activation of nuclear receptors, oxidative stress, and PPAR signalling. Below, a selection of matches observed (or

Table 2A
Maximum scores obtained across concentrations in the rat primary hepatocyte dataset.

AM	APAP	AZP	CBZ	CFB	CPA	CPZ	CSA	DFNa	ETH	ETP	FFB	IBU	PH	RIF	TUN	VPA	WY
IBU: 314	FFB: 114	PH: 573	CPZ: 310	WY: 1244	ETP: 429	PH: 420	RIF: 656	CFB: 710	CBZ: 199	RIF: 747	CFB: 1212	FFB: 1079	AZP: 573	ETP: 747	DFNa: 247	WY: 1070	CFB: 1244
FFB: 292	CFB: 112	CPZ: 367	PH: 260	FFB: 1212	CPZ: 225	AZP: 367	ETP: 386	FFB: 652	CSA: 150	CPA: 429	WY: 1205	CFB: 1056	CPZ: 420	CSA: 656	CSA: 158	CFB: 1002	FFB: 1205
WY: 266	VPA: 111	CSA: 349	ETP: 244	IBU: 1056	CBZ: 212	CSA: 337	AZP: 349	IBU: 601	TUN: 143	CSA: 386	IBU: 1079	WY: 1056	CSA: 339	IBU: 352	ETH: 143	FFB: 970	VPA: 1070
CFB: 232	IBU: 102	ETP: 166	CPA: 212	VPA: 1002	CSA: 208	CBZ: 310	PH: 339	VPA: 591	PH: 112	IBU: 300	VPA: 970	VPA: 908	CBZ: 260	DFNa: 258	AZP: 139	IBU: 908	IBU: 1056
VPA: 213	WY: 96	DFNa: 147	ETH: 199	DFNa: 710	DFNa: 132	CPA: 225	CPZ: 337	WY: 482	IBU: 109	DFNa: 280	DFNa: 652	DFNa: 601	DFNa: 209	PH: 163	IBU: 133	DFNa: 591	DFNa: 482
CPZ: 121	DFNa: 94	TUN: 139	RIF: 127	AM: 232	PH: 107	ETP: 216	DFNa: 283	CSA: 283	AM: 103	VPA: 259	AM: 292	RIF: 352	IBU: 192	CPZ: 161	VPA: 123	ETP: 259	AM: 266
ETH: 103	ETH: 89	RIF: 133	DFNa: 122	APAP: 112	RIF: 83	DFNa: 163	IBU: 275	ETP: 280	CPZ: 90	CBZ: 244	APAP: 114	AM: 314	ETP: 172	AZP: 133	CPZ: 98	AM: 213	APAP: 96
DFNa: 95	CSA: 76	IBU: 101	CSA: 112	TUN: 49	ETH: 71	RIF: 161	CPA: 208	RIF: 258	APAP: 89	CPZ: 216	PH: 87	ETP: 300	RIF: 163	CBZ: 127	CBZ: 70	CSA: 153	ETP: 44

Table 2B
Maximum scores obtained across concentrations in the human primary hepatocyte dataset.

AM	APAP	AZP	CBZ	CFB	CPA	CPZ	CSA	DFNa	ETH	ETP	FFB	IBU	PH	RIF	TUN	VPA	WY
CPZ: 199	DFNa: 551	ETP: 675	CPA: 910	WY: 780	CBZ: 910	CBZ: 630	ETP: 842	ETP: 690	ETP: 348	CSA: 842	CFB: 739	FFB: 650	CPZ: 566	CPA: 839	CSA: 561	ETH: 326	CFB: 780
CBZ: 198	AZP: 479	DFNa: 501	CPZ: 630	FFB: 739	RIF: 839	PH: 566	TUN: 561	APAP: 551	DFNa: 332	DFNa: 690	IBU: 650	WY: 410	CBZ: 416	WY: 649	ETP: 531	CBZ: 296	RIF: 649
CPA: 166	ETP: 469	APAP: 479	RIF: 608	IBU: 346	WY: 542	CPA: 447	DFNa: 521	CPA: 536	VPA: 326	AZP: 675	WY: 585	CFB: 346	CPA: 185	CBZ: 608	DFNa: 433	RIF: 291	FFB: 585
RIF: 166	CSA: 335	CSA: 433	WY: 463	VPA: 266	DFNa: 536	WY: 382	AZP: 433	CSA: 521	CSA: 303	TUN: 531	VPA: 152	DFNa: 144	AZP: 183	DFNa: 508	APAP: 290	CFB: 266	CPA: 542
DFNa: 128	TUN: 290	TUN: 286	PH: 416	DFNa: 188	CPZ: 447	RIF: 302	APAP: 335	RIF: 508	APAP: 274	APAP: 469	RIF: 106	AZP: 127	DFNa: 146	CPZ: 302	AZP: 286	ETP: 238	CBZ: 463
WY: 127	ETH: 274	ETH: 223	VPA: 296	AZP: 137	VPA: 237	AM: 199	ETH: 303	AZP: 501	AZP: 223	ETH: 348	AZP: 95	VPA: 105	APAP: 143	VPA: 291	VPA: 228	CPA: 237	IBU: 410
PH: 96	VPA: 213	VPA: 208	DFNa: 277	RIF: 108	ETH: 208	DFNa: 181	VPA: 198	TUN: 433	TUN: 223	VPA: 238	ETH: 94	CPA: 96	TUN: 104	APAP: 181	ETH: 223	TUN: 228	CPZ: 382
VPA: 78	CBZ: 204	CPA: 185	APAP: 204	ETH: 92	APAP: 192	ETH: 147	PH: 94	ETH: 332	CPA: 208	CPA: 118	CPA: 66	ETP: 88	AM: 96	AM: 166	WY: 125	DFNa: 225	DFNa: 313

lack thereof) in primary human and rat hepatocytes is discussed based on overlapping MOAs.

4.1. DNA damage

An example of an expected but missing match is a match between etoposide (ETP), a well-known topoisomerase II inhibitor and Cyclophosphamide (CPA). Topoisomerase II inhibitors such as ETP, induce DNA double stranded breaks leading to apoptosis through transient stabilization of the topoisomeriase IIα-DNA complex (Choudhury et al., 2004). Also CPA induces DNA strand breaks, however single stranded, through the formation of DNA-DNA crosslinks, leading to inhibition of DNA synthesis and cell apoptosis (Kawabata et al., 1990; Murata et al., 2004). Based on their large overlap in MOA, a match between these two compounds would be expected. Such a match, however, was absent in primary human hepatocytes and only present to a limited extent in primary rat hepatocytes (score 429, < 10 hits). The limited capability of detecting genotoxic modes of action in primary hepatocytes was also apparent in our previous study, which involved primary mouse hepatocytes and mouse embryonic stem cells (Schaap et al., 2015). Although the absence of a match can be explained by the post-mitotic state of the primary hepatocytes used, pathway analysis (Supplemental File 3 and 4) still showed a number of significantly regulated pathways related to DNA replication and DNA repair as well as cell cycle regulation and cellular senescence in both rat and human. This clearly indicates that at least part of the MOA is detected despite the apparent limitations of the model system.

4.2. P53-mediated pathways

In primary human hepatocytes, a match between ETP and cyclosporine A (CSA; score 842), diclofenac (DFNa; score 690), azathioprine (AZP; score 675) and tunicamycin (TUN; score 531) was identified. Although pathway analysis (Supplemental file 4) indicated that all matches observed for ETP converge on a p53-dependent MOA, different underlying mechanisms can be identified indicative of only partially overlapping MOAs. As an example, the match between ETP and AZP is based on the observation that ETP exposure induces apoptosis through a p53-dependent pathway involving mitochondrial stress and the release of mitochondrial Cytochrome C (Choudhury et al., 2004; Karpinich et al., 2002). Azathioprine (AZP) on the other hand causes reactive oxygen species (ROS)-induced DNA- and mitochondrial damage leading to (p53-dependent) cell-cycle arrest and apoptosis (Karran, 2006). This occurs through the formation of oxidation-prone and immunosuppressive 6-thioguanine metabolites (6-TG) (Sahasranaman et al., 2008). The observation that the toxicity of both ETP and AZP relies on DNA-related mechanisms is illustrated by the presence of significantly enriched pathways predominantly related to DNA repair mechanisms, DNA replication and cell cycle (Supplemental file 4).

4.3. Endoplasmic reticulum-stress

Partial overlap with a different MOA is underlying the match between ETP and both CSA and TUN. For CSA, in vitro as well as in vivo studies have demonstrated induction of apoptosis via sustained endoplasmic reticulum (ER) stress, activation of the unfolded-protein response (UPR) and mitochondrial dysfunction (Korolczuk et al., 2016; Szalowska et al., 2013). Comparably, TUN exposure is known to induce ER-stress and UPR, though depending on downregulation of pathways involved in lipid synthesis and inhibition of metabolic pathways (Malhi and Kaufman, 2011). ER-stress- and UPR-related cell death in hepatocytes has been shown to depend on mitochondrial pathways regulated via the B cell lymphoma 2 (BCL-2) protein family and the closely connected p53 (Hemann and Lowe, 2006; Hetz, 2012).

Indeed, pathway analysis for CSA, TUN and ETP showed convergence on pathways involved in p53-associated mechanisms including cell cycle regulation and several DNA repair mechanisms. Additionally, both CSA and TUN showed significantly enriched pathways involved in ER-stress such as protein export and protein processing in endoplasmic reticulum for both TUN and CSA. These pathways are absent for ETP (Supplemental file 4). The observation of a comparable, though much weaker, match between ETP and CSA in rat hepatocytes (score 386 versus 842; Table 2A; 2B) indicates a difference in species sensitivity for these mechanisms (Supplemental file 3).

4.4. Nuclear receptors and species differences

The match between ETP and DFNa in primary human hepatocytes is based on overlap in p53-related cell cycle regulation and metabolic pathways at the high doses of DFNa and ETP (Supplemental file 2). In contrast to pharmaceutical (non-toxic) doses of DFNa (Sinz et al., 2006; Tang, 2003), high doses of DFNa may saturate normal elimination routes and result in radical-prone metabolism by peroxidases disrupting the mitochondrial respiratory chain causing p53-mediated apoptotic or necrotic cell death (Boelsterli, 2003; Nouri et al., 2017). Our pathway analysis indeed displays an overlap between ETP and DFNa based on p53-related cell cycle regulation and metabolic pathways. However, the emergence of additional significantly enriched pathways related to RXR-related pathways, drug metabolism as well as mitochondrial dysfunction and programmed cell death in the human data with DFNa. as opposed to the DNA damage- and repair-related pathways observed

with ETP, illustrates that the overlap in MOAs between ETP and DFNa is only partial (Supplemental files 3 and 4).

In rat primary hepatocytes, a strong match between ETP and DFNa is absent (max score 280; Table 2A). This is in line with findings by Lauer and co-workers who demonstrated a comparable mechanism in rat and human hepatocytes, but report a higher sensitivity for human- compared to rat hepatocytes (Lauer et al., 2009). This difference in sensitivity could be explained by the induction of metabolism via binding of DFNa to the Pregnane X Receptor (PXR) in human hepatocytes, which does not occur in rat (LeCluyse, 2001; Tirona et al., 2004). This species difference is also apparent in our pathway analysis where human data does include significant enrichment of RXR-related pathways (Supplemental file 4) whereas rat data shows no regulation of PXR or RXR-related pathways (Supplemental file 3).

Comparably, RIF has been shown to activate human PXR, but not rat PXR (LeCluyse, 2001; Tirona et al., 2004). This is reflected in the observation that RIF matched with CPA, WY-14,643 (WY), carbamazepine (CBZ) and DFNa in human hepatocytes, converging on PXR-related pathways (Supplemental file 4) whereas these pathways were absent in the matches observed in rat hepatocytes (ETP and CSA; Supplemental file 3). In general, PXR activation leads to upregulated expression of phase I and II drug metabolizing enzymes, such as cytochrome P450 enzymes (CYPs), glutathione S-transferases (GSTs), N-acetyl transferases (NATs) and transporters (involved in phase III) (Mackowiak and Wang, 2016; Willson and Kliewer, 2002). This is in turn related to induction of the production of excessive reactive oxygen species (ROS) leading to lipid peroxidation and cell death.

4.5. Oxidative stress

Activation of Nrf2, a widely recognized master regulator of cellular redox homeostasis, counteracts the increased ROS production in mitochondria (Liu et al., 2013). However, recent studies suggest reciprocal regulation of the Nrf2 and PPARγ signalling pathways to reinforce the oxidative stress response (Huang et al., 2010; Lee, 2017). Herein, PPARγ, a target gene of Nrf2 (Huang et al., 2010), has been identified as negative regulator of oxidative stress-induced inflammation (Lee, 2017). The induction of oxidative stress and subsequent activation of the Nrf2 and PPARγ signalling pathways thus likely explains the matches between RIF, CPA, CBZ and DFNa in human hepatocytes (Alqahtani and Mahmoud, 2016; Herpers et al., 2016; Higuchi et al., 2012; Jamis-Dow et al., 1997; Kim et al., 2017; Li and Chiang, 2006; Nakajima et al., 2011; Ramappa and Aithal, 2013; Wang et al., 2016; Zhou et al., 2006). The resulting pro-apoptotic signalling induced by pro-inflammatory cytokines is reflected in pathways such as TNF signalling, MAPK signalling, NF-κB signalling and apoptosis (Supplemental Files 3 and 4).

4.6. PPAR signalling

As expected, PPARα agonists WY, CFB and FFB grouped robustly in both primary rat hepatocytes and primary human hepatocytes (Table 2A and 2B) converging on activation of PPAR signalling, as illustrated by significant enrichment of several pathways related to PPAR signalling, peroxisome activation and fatty acid turnover (Supplemental file 3 and 4). Additional grouping with IBU, DFNa and VPA, was observed in rat cells (Table 2A). In human cells however, only weak matches were observed between the PPARα agonists, IBU and DFNa while the match with VPA was absent (Table 2B). The observed match between PPAR alpha agonists and IBU (Table 2A and 2B) can be explained by the observation that NSAIDs, such as IBU, may act as PPARγ agonist (Lehmann et al., 1997; Puhl et al., 2015). Considering the close ties between the different PPAR signalling pathways and COX-inhibition, which is the primary mode of action of NSAIDs, this provides a rationale for the grouping of NSAIDs with PPARα agonists. Indeed, pathway analysis for IBU in both rat and human displays significant regulation of PPAR signalling-related pathways comparable to the PPARα agonists although much stronger in rat compared to human. Also for DFNa, a clear match is observed with the PPARα agonists based on regulation of PPAR-signalling pathways, though only in rat (Table 2A and 2B). Comparably, VPA showed a consistent strong match with PPARα agonists as well as IBU and DFNa in rat, but not in human, converging on PPAR signalling, peroxisome activation and fatty acid turnover.

Although PPAR agonism is detected in both human and rat primary hepatocytes, species differences lead to a far lower responsiveness to PPAR agonists in test systems based on human cells compared to rat (Corton et al., 2014; Liss and Finck, 2017; Okyere et al., 2014). In the TG-GATEs dataset, this lower responsiveness is likely reflected in the far lower number of differential expressed genes in response to PPARα agonist exposure observed in human primary hepatocytes (data not shown).

The basis for the match between RIF and WY in human hepatocytes is their effect on lipid peroxidation. WY is a typical PPARα agonist, which is known to transcriptionally activate genes that participate in peroxisomal, microsomal, and mitochondrial fatty acid oxidation. RIF exposure on the other hand, leads to increased lipid peroxidation through the activation of PXR and induction of ROS (Begriche et al., 2011; Lee et al., 2003). This MOA was reflected in the enrichment of pathways such as PPAR signalling, peroxisome, and fatty acid degradation (Supplemental file 4). Additionally, both compounds affect bile acid formation via nuclear receptor signalling cascades in turn affecting the transcription of hepatocyte transporter genes critical for bile formation, e.g. the bile salt export pump (Chen et al., 2014; Guo et al., 2015; Kullak-Ublick and Becker, 2003; Pineda Torra et al., 2003; Staudinger et al., 2013; Wang et al., 2014).

4.7. Overall performance

For the dataset studied, we demonstrated that further development of the comparison approach rendered general applicability, while it is still capable of recognizing presence or absence of overlaps in MOA. The various examples discussed above show that also a partial overlap in MOA is detected. Nevertheless, a few issues remain that need to be resolved. Above all, the current version of the comparison approach produces best matches across the concentrations or doses tested, but possible concentration-response relationships need to be checked manually. Automated generation of this information would be highly valuable, as it would strongly facilitate interpretation of results. This also applies to the analysis of differentially regulated pathways since the examples of matches discussed indicate that the output of the comparison approach cannot be interpreted correctly solely based on matches at the gene level.

Besides the comparison approach itself, test conditions, including selection of the test concentrations, exposure duration and choice of model(s), remain highly important. This is illustrated here by AM, for which the absence of matches appears related to choice of test concentrations, as well as the differential outcomes from human and rat cells. Also, to what extent intrinsic aspects of the cell model such as genetic background and sex play a role requires further investigation. Based on the outcomes of the present and previous studies, we propose to employ multiple in vitro testing systems that complement each other in their characteristics, e.g. biotransformation capacity, cell type, proliferation etc. Ultimately, an optimal combination of robust test systems needs to produce reliable outcomes that are, without exceptions, relevant to human health risk assessment. While searching for this combination, the use of cell systems from different species could be of added value. Including test systems derived from different species will inform on the one hand on the usefulness of a particular test system (results are consistent with those obtained from other test systems) whilst on the other hand species-specific results will indicate which test system produces results that are relevant to human health risk

assessment.

5. Conclusion

Taken together, we demonstrated that the new version of the comparison approach is an unbiased approach to inform on the MOA(s) of a chemical of interest. We consider this approach complementary to other data sources, such as the ToxCast database (Judson et al., 2010; Richard et al., 2016; Tice et al., 2013). Where High-Throughput Screening approaches such as ToxCast mainly inform on molecular initiating events, the comparison approach takes a broader perspective and provides a more complex understanding of the MOA with information on key events, which may support the development of AOPs. This renders the comparison approach a useful tool for mechanism-based risk assessment.

Conflicts of interest

The authors declare they have no conflict of interest.

Acknowledgements

We are grateful to Eric Gremmer for the manuscript's artwork, Harry van Steeg for valuable discussions and Jan van Benthem for his expert input. This study has been performed by order and for the account of The Netherlands Ministry of Health, Welfare and Sports.

Appendix A. Supplementary data

Supplementary data related to this article can be found at https://doi.org/10.1016/j.fct.2018.08.007.

Transparency document

Transparency document related to this article can be found online at https://doi.org/10.1016/j.fct.2018.08.007.

References

Alqahtani, S., Mahmoud, A.M., 2016. Gamma-glutamylcysteine ethyl ester protects against cyclophosphamide-induced liver injury and hematologic alterations via up-regulation of PPARgamma and attenuation of oxidative stress, inflammation, and apoptosis. Oxid Med Cell Longev 2016, 4016209. https://doi.org/10.1155/2016/4016209.

Angrish, M.M., Kaiser, J.P., McQueen, C.A., Chorley, B.N., 2016. Tipping the balance: hepatotoxicity and the 4 apical key events of hepatic steatosis. Toxicol. Sci. : an official journal of the Society of Toxicology 150 (2), 261–268. https://doi.org/10.1093/toxsci/kfw018.

Ankley, G.T., Bennett, R.S., Erickson, R.J., et al., 2010. Adverse outcome pathways: a conceptual framework to support ecotoxicology research and risk assessment. Environ. Toxicol. Chem. 29 (3), 730–741. https://doi.org/10.1002/etc.34.

Antherieu, S., Bachour-El Azzi, P., Dumont, J., et al., 2013. Oxidative stress plays a major role in chlorpromazine-induced cholestasis in human HepaRG cells. Hepatology 57 (4), 1518–1529. https://doi.org/10.1002/hep.26160.

Begriche, K., Massart, J., Robin, M.A., Borgne-Sanchez, A., Fromenty, B., 2011. Drug-induced toxicity on mitochondria and lipid metabolism: mechanistic diversity and deleterious consequences for the liver. J. Hepatol. 54 (4), 773–794. https://doi.org/10.1016/j.jhep.2010.11.006.

Bessone, F., 2010. Non-steroidal anti-inflammatory drugs: what is the actual risk of liver damage? World J. Gastroenterol. 16 (45), 5651. https://doi.org/10.3748/wjg.v16.i45.5651.

Boelsterli, U., 2003. Diclofenac-induced liver injury: a paradigm of idiosyncratic drug toxicity. Toxicol. Appl. Pharmacol. 192 (3), 307–322. https://doi.org/10.1016/s0041-008x(03)00368-5.

Carlson, M.R., Pages, H., Arora, S., Obenchain, V., Morgan, M., 2016. Genomic annotation resources in R/Bioconductor. Meth. Mol. Biol. 1418, 67–90. https://doi.org/10.1007/978-1-4939-3578-9_4.

Chen, J., Zhao, K.N., Chen, C., 2014. The role of CYP3A4 in the biotransformation of bile acids and therapeutic implication for cholestasis. Ann. Transl. Med. 2 (1), 7. https://doi.org/10.3978/j.issn.2305-5839.2013.03.02.

Choudhury, R.C., Palo, A.K., Sahu, P., 2004. Cytogenetic risk assessment of etoposide from mouse bone marrow. J. Appl. Toxicol. : JAT (J. Appl. Toxicol.) 24 (2), 115–122. https://doi.org/10.1002/jat.959.

Corton, J.C., Cunningham, M.L., Hummer, B.T., et al., 2014. Mode of action framework analysis for receptor-mediated toxicity: the peroxisome proliferator-activated receptor alpha (PPARalpha) as a case study. Crit. Rev. Toxicol. 44 (1), 1–49. https://doi.org/10.3109/10408444.2013.835784.

DeLeve, L.D., 1996. Cellular target of cyclophosphamide toxicity in the murine liver: role of glutathione and site of metabolic activation. Hepatology 24 (4), 830–837. https://doi.org/10.1002/hep.510240414.

Elshater, A.A., Haridy, M.A.M., Salman, M.M.A., Fayyad, A.S., Hammad, S., 2017. Fullerene C60 nanoparticles ameliorated cyclophosphamide-induced acute hepatotoxicity in rats. Biomed. Pharmacother. 97, 53–59. https://doi.org/10.1016/j.biopha.2017.10.134.

Foufelle, F., Fromenty, B., 2016. Role of endoplasmic reticulum stress in drug-induced toxicity. Pharmacol Res Perspect 4 (1), e00211. https://doi.org/10.1002/prp2.211.

Fredriksson, L., Wink, S., Herpers, B., et al., 2014. Drug-induced endoplasmic reticulum and oxidative stress responses independently sensitize toward TNFalpha-mediated hepatotoxicity. Toxicol. Sci. : an official journal of the Society of Toxicology 140 (1), 144–159. https://doi.org/10.1093/toxsci/kfu072.

Grigorian, A., O'Brien, C.B., 2014. Hepatotoxicity secondary to chemotherapy. J Clin Transl Hepatol 2 (2), 95–102. https://doi.org/10.14218/JCTH.2014.00011.

Guo, Y.X., Xu, X.F., Zhang, Q.Z., et al., 2015. The inhibition of hepatic bile acids transporters Ntcp and Bsep is involved in the pathogenesis of isoniazid/rifampicin-induced hepatotoxicity. Toxicol. Mech. Meth. 25 (5), 382–387. https://doi.org/10.3109/15376516.2015.1033074.

Hanahan, D., Weinberg, R.A., 2000. The hallmarks of cancer. Cell 100 (1), 57–70.

Hanahan, D., Weinberg, R.A., 2011. Hallmarks of cancer: the next generation. Cell 144 (5), 646–674. https://doi.org/10.1016/j.cell.2011.02.013.

Hemann, M.T., Lowe, S.W., 2006. The p53-Bcl-2 connection. Cell Death Differ. 13 (8), 1256–1259. https://doi.org/10.1038/sj.cdd.4401962.

Henderson, M.C., Siddens, L.K., Morre, J.T., Krueger, S.K., Williams, D.E., 2008. Metabolism of the anti-tuberculosis drug ethionamide by mouse and human FMO1, FMO2 and FMO3 and mouse and human lung microsomes. Toxicol. Appl. Pharmacol. 233 (3), 420–427. https://doi.org/10.1016/j.taap.2008.09.017.

Hernandez, L.G., van Steeg, H., Luijten, M., van Benthem, J., 2009. Mechanisms of non-genotoxic carcinogens and importance of a weight of evidence approach. Mutat. Res. 682 (2–3), 94–109. https://doi.org/10.1016/j.mrrev.2009.07.002.

Herpers, B., Wink, S., Fredriksson, L., et al., 2016. Activation of the Nrf2 response by intrinsic hepatotoxic drugs correlates with suppression of NF-kappaB activation and sensitizes toward TNFalpha-induced cytotoxicity. Arch. Toxicol. 90 (5), 1163–1179. https://doi.org/10.1007/s00204-015-1536-3.

Hetz, C., 2012. The unfolded protein response: controlling cell fate decisions under ER stress and beyond. Nat. Rev. Mol. Cell Biol. 13 (2), 89–102. https://doi.org/10.1038/nrm3270.

Higuchi, S., Yano, A., Takai, S., et al., 2012. Metabolic activation and inflammation reactions involved in carbamazepine-induced liver injury. Toxicol. Sci.: an official journal of the Society of Toxicology 130 (1), 4–16. https://doi.org/10.1093/toxsci/kfs222.

Huang, J., Tabbi-Anneni, I., Gunda, V., Wang, L., 2010. Transcription factor Nrf2 regulates SHP and lipogenic gene expression in hepatic lipid metabolism. Am. J. Physiol. Gastrointest. Liver Physiol. 299 (6), G1211–G1221. https://doi.org/10.1152/ajpgi.00322.2010.

Igarashi, Y., Nakatsu, N., Yamashita, T., et al., 2015. Open TG-GATEs: a large-scale toxicogenomics database. Nucleic Acids Res. 43 (Database issue), D921–D927. https://doi.org/10.1093/nar/gku955.

Iida, A., Sasaki, E., Yano, A., et al., 2015. Carbamazepine-induced liver injury requires CYP3A-mediated metabolism and glutathione depletion in rats. Drug Metabol. Dispos.: the biological fate of chemicals 43 (7), 958–968. https://doi.org/10.1124/dmd.115.063370.

Irizarry, R.A., Bolstad, B.M., Collin, F., Cope, L.M., Hobbs, B., Speed, T.P., 2003. Summaries of Affymetrix GeneChip probe level data. Nucleic Acids Res. 31 (4), e15.

Jacobs, M.N., Colacci, A., Louekari, K., et al., 2016. International regulatory needs for development of an IATA for non-genotoxic carcinogenic chemical substances. ALTEX. https://doi.org/10.14573/altex.1601201.

Jamis-Dow, C.A., Katki, A.G., Collins, J.M., Klecker, R.W., 1997. Rifampin and rifabutin and their metabolism by human liver esterases. Xenobiotica; the fate of foreign compounds in biological systems 27 (10), 1015–1024. https://doi.org/10.1080/004982597239994.

Judson, R.S., Houck, K.A., Kavlock, R.J., et al., 2010. In vitro screening of environmental chemicals for targeted testing prioritization: the ToxCast project. Environ. Health Perspect. 118 (4), 485–492. https://doi.org/10.1289/ehp.0901392.

Karpinich, N.O., Tafani, M., Rothman, R.J., Russo, M.A., Farber, J.L., 2002. The course of etoposide-induced apoptosis from damage to DNA and p53 activation to mitochondrial release of cytochrome c. J. Biol. Chem. 277 (19), 16547–16552. https://doi.org/10.1074/jbc.M110629200.

Karran, P., 2006. Thiopurines, DNA damage, DNA repair and therapy-related cancer. Br. Med. Bull. 79–80, 153–170. https://doi.org/10.1093/bmb/ldl020.

Kawabata, T.T., Chapman, M.Y., Kim, D.H., Stevens, W.D., Holsapple, M.P., 1990. Mechanisms of in vitro immunosuppression by hepatocyte-generated cyclophosphamide metabolites and 4-hydroperoxycyclophosphamide. Biochem. Pharmacol. 40 (5), 927–935.

Kim, J.H., Nam, W.S., Kim, S.J., et al., 2017. Mechanism investigation of rifampicin-induced liver injury using comparative toxicoproteomics in mice. Int. J. Mol. Sci. 18 (7). https://doi.org/10.3390/ijms18071417.

Korolczuk, A., Caban, K., Amarowicz, M., Czechowska, G., Irla-Miduch, J., 2016. Oxidative stress and liver morphology in experimental cyclosporine a-induced hepatotoxicity. BioMed Res. Int. 2016, 5823271. https://doi.org/10.1155/2016/5823271.

Kullak-Ublick, G.A., Becker, M.B., 2003. Regulation of drug and bile salt transporters in

liver and intestine. Drug Metab. Rev. 35 (4), 305–317. https://doi.org/10.1081/DMR-120026398.
Lampen, A., Carlberg, C., Nau, H., 2001. Peroxisome proliferator-activated receptor δ is a specific sensor for teratogenic valproic acid derivatives. Eur. J. Pharmacol. 431 (1), 25–33. https://doi.org/10.1016/s0014-2999(01)01423-6.
Lauer, B., Tuschl, G., Kling, M., Mueller, S.O., 2009. Species-specific toxicity of diclofenac and troglitazone in primary human and rat hepatocytes. Chem. Biol. Interact. 179 (1), 17–24. https://doi.org/10.1016/j.cbi.2008.10.031.
LeCluyse, E.L., 2001. Pregnane X receptor: molecular basis for species differences in CYP3A induction by xenobiotics. Chem. Biol. Interact. 134 (3), 283–289.
Lee, C., 2017. Collaborative power of Nrf2 and PPARgamma activators against metabolic and drug-induced oxidative injury. Oxid Med Cell Longev 2017, 1378175. https://doi.org/10.1155/2017/1378175.
Lee, C.H., Olson, P., Evans, R.M., 2003. Minireview: lipid metabolism, metabolic diseases, and peroxisome proliferator-activated receptors. Endocrinology 144 (6), 2201–2207. https://doi.org/10.1210/en.2003-0288.
Lehmann, J.M., Lenhard, J.M., Oliver, B.B., Ringold, G.M., Kliewer, S.A., 1997. Peroxisome proliferator-activated receptors alpha and gamma are activated by indomethacin and other non-steroidal anti-inflammatory drugs. J. Biol. Chem. 272 (6), 3406–3410.
Li, T., Chiang, J.Y., 2006. Rifampicin induction of CYP3A4 requires pregnane X receptor cross talk with hepatocyte nuclear factor 4alpha and coactivators, and suppression of small heterodimer partner gene expression. Drug Metabol. Dispos.: the biological fate of chemicals 34 (5), 756–764. https://doi.org/10.1124/dmd.105.007575.
Liss, K.H., Finck, B.N., 2017. PPARs and nonalcoholic fatty liver disease. Biochimie 136, 65–74. https://doi.org/10.1016/j.biochi.2016.11.009.
Liu, J., Wu, K.C., Lu, Y.F., Ekuase, E., Klaassen, C.D., 2013. Nrf2 protection against liver injury produced by various hepatotoxicants. Oxid Med Cell Longev 2013, 305861. https://doi.org/10.1155/2013/305861.
Mackowiak, B., Wang, H., 2016. Mechanisms of xenobiotic receptor activation: direct vs. indirect. Biochim. Biophys. Acta 1859 (9), 1130–1140. https://doi.org/10.1016/j.bbagrm.2016.02.006.
Malhi, H., Kaufman, R.J., 2011. Endoplasmic reticulum stress in liver disease. J. Hepatol. 54 (4), 795–809. https://doi.org/10.1016/j.jhep.2010.11.005.
Meek, M.E., Boobis, A., Cote, I., et al., 2014. New developments in the evolution and application of the WHO/IPCS framework on mode of action/species concordance analysis. J. Appl. Toxicol. : JAT (J. Appl. Toxicol.) 34 (1), 1–18. https://doi.org/10.1002/jat.2949.
Meek, M.E., Bucher, J.R., Cohen, S.M., et al., 2003. A framework for human relevance analysis of information on carcinogenic modes of action. Crit. Rev. Toxicol. 33 (6), 591–653. https://doi.org/10.1080/713608373.
Murata, M., Suzuki, T., Midorikawa, K., Oikawa, S., Kawanishi, S., 2004. Oxidative DNA damage induced by a hydroperoxide derivative of cyclophosphamide. Free Radic. Biol. Med. 37 (6), 793–802. https://doi.org/10.1016/j.freeradbiomed.2004.05.009.
Nakajima, A., Fukami, T., Kobayashi, Y., Watanabe, A., Nakajima, M., Yokoi, T., 2011. Human arylacetamide deacetylase is responsible for deacetylation of rifamycins: rifampicin, rifabutin, and rifapentine. Biochem. Pharmacol. 82 (11), 1747–1756. https://doi.org/10.1016/j.bcp.2011.08.003.
Nouri, A., Heidarian, E., Nikoukar, M., 2017. Effects of N-acetyl cysteine on oxidative stress and TNF-alpha gene expression in diclofenac-induced hepatotoxicity in rats. Toxicol. Mech. Meth. 27 (8), 561–567. https://doi.org/10.1080/15376516.2017.1334732.
Okyere, J., Oppon, E., Dzidzienyo, D., Sharma, L., Ball, G., 2014. Cross-species gene expression analysis of species specific differences in the preclinical assessment of pharmaceutical compounds. PLoS One 9 (5), e96853. https://doi.org/10.1371/journal.pone.0096853.
Phipson, B., Lee, S., Majewski, I.J., Alexander, W.S., Smyth, G.K., 2016. Robust hyperparameter estimation protects against hypervariable genes and improves power to detect differential expression. Ann. Appl. Stat. 10 (2), 946–963. https://doi.org/10.1214/16-AOAS920.
Pineda Torra, I., Claudel, T., Duval, C., Kosykh, V., Fruchart, J.C., Staels, B., 2003. Bile acids induce the expression of the human peroxisome proliferator-activated receptor alpha gene via activation of the farnesoid X receptor. Mol. Endocrinol. 17 (2), 259–272. https://doi.org/10.1210/me.2002-0120.
Puhl, A.C., Milton, F.A., Cvoro, A., et al., 2015. Mechanisms of peroxisome proliferator activated receptor gamma regulation by non-steroidal anti-inflammatory drugs. Nucl. Recept. Signal. 13, e004. https://doi.org/10.1621/nrs.13004.
Ramappa, V., Aithal, G.P., 2013. Hepatotoxicity related to anti-tuberculosis drugs: mechanisms and management. J Clin Exp Hepatol 3 (1), 37–49. https://doi.org/10.1016/j.jceh.2012.12.001.
Reyes-Gordillo, K., Shah, R., Muriel, P., 2017. Oxidative stress and inflammation in hepatic diseases: current and future therapy. Oxid Med Cell Longev 2017, 3140673. https://doi.org/10.1155/2017/3140673.
Richard, A.M., Judson, R.S., Houck, K.A., et al., 2016. ToxCast chemical landscape: paving the road to 21st century toxicology. Chem. Res. Toxicol. 29 (8), 1225–1251. https://doi.org/10.1021/acs.chemrestox.6b00135.
Sahasranaman, S., Howard, D., Roy, S., 2008. Clinical pharmacology and pharmacogenetics of thiopurines. Eur. J. Clin. Pharmacol. 64 (8), 753–767. https://doi.org/10.1007/s00228-008-0478-6.
Schaap, M.M., Wackers, P.F., Zwart, E.P., et al., 2015. A novel toxicogenomics-based approach to categorize (non-)genotoxic carcinogens. Arch. Toxicol. 89 (12), 2413–2427. https://doi.org/10.1007/s00204-014-1368-6.
Schaap, M.M., Zwart, E.P., Wackers, P.F., et al., 2012. Dissecting modes of action of non-genotoxic carcinogens in primary mouse hepatocytes. Arch. Toxicol. 86 (11), 1717–1727. https://doi.org/10.1007/s00204-012-0883-6.
Selim, K., Kaplowitz, N., 1999. Hepatotoxicity of psychotropic drugs. Hepatology 29 (5), 1347–1351. https://doi.org/10.1002/hep.510290535.
Sinz, M., Kim, S., Zhu, Z., et al., 2006. Evaluation of 170 xenobiotics as transactivators of human pregnane X receptor (hPXR) and correlation to known CYP3A4 drug interactions. Curr. Drug Metabol. 7 (4), 375–388. https://doi.org/10.2174/138920006776873535.
Sonich-Mullin, C., Fielder, R., Wiltse, J., et al., 2001. IPCS conceptual framework for evaluating a mode of action for chemical carcinogenesis. Regul. Toxicol. Pharmacol. : RTP (Regul. Toxicol. Pharmacol.) 34 (2), 146–152. https://doi.org/10.1006/rtph.2001.1493.
Staudinger, J.L., Woody, S., Sun, M., Cui, W., 2013. Nuclear-receptor-mediated regulation of drug- and bile-acid-transporter proteins in gut and liver. Drug Metab. Rev. 45 (1), 48–59. https://doi.org/10.3109/03602532.2012.748793.
Sutherland, J.J., Webster, Y.W., Willy, J.A., et al., 2017. Toxicogenomic module associations with pathogenesis: a network-based approach to understanding drug toxicity. Pharmacogenomics J. https://doi.org/10.1038/tpj.2017.17.
Szalowska, E., Stoopen, G., Groot, M.J., Hendriksen, P.J., Peijnenburg, A.A., 2013. Treatment of mouse liver slices with cholestatic hepatotoxicants results in down-regulation of Fxr and its target genes. BMC Med. Genom. 6, 39. https://doi.org/10.1186/1755-8794-6-39.
Tang, W., 2003. The metabolism of diclofenac - enzymology and toxicology perspectives. Curr. Drug Metabol. 4 (4), 319–329. https://doi.org/10.2174/1389200033489398.
Tapner, M.J., Jones, B.E., Wu, W.M., Farrell, G.C., 2004. Toxicity of low dose azathioprine and 6-mercaptopurine in rat hepatocytes. Roles of xanthine oxidase and mitochondrial injury. J. Hepatol. 40 (3), 454–463. https://doi.org/10.1016/j.jhep.2003.11.024.
Tice, R.R., Austin, C.P., Kavlock, R.J., Bucher, J.R., 2013. Improving the human hazard characterization of chemicals: a Tox21 update. Environ. Health Perspect. 121 (7), 756–765. https://doi.org/10.1289/ehp.1205784.
Tirona, R.G., Leake, B.F., Podust, L.M., Kim, R.B., 2004. Identification of amino acids in rat pregnane X receptor that determine species-specific activation. Mol. Pharmacol. 65 (1), 36–44. https://doi.org/10.1124/mol.65.1.36.
van de Water, F.M., Havinga, J., Ravesloot, W.T., Horbach, G.J., Schoonen, W.G., 2011. High content screening analysis of phospholipidosis: validation of a 96-well assay with CHO-K1 and HepG2 cells for the prediction of in vivo based phospholipidosis. Toxicol. Vitro : an international journal published in association with BIBRA 25 (8), 1870–1882. https://doi.org/10.1016/j.tiv.2011.05.026.
Vinken, M., Landesmann, B., Goumenou, M., et al., 2013. Development of an adverse outcome pathway from drug-mediated bile salt export pump inhibition to cholestatic liver injury. Toxicol. Sci. : an official journal of the Society of Toxicology 136 (1), 97–106. https://doi.org/10.1093/toxsci/kft177.
Wang, C., Fan, R.Q., Zhang, Y.X., Nie, H., Li, K., 2016. Naringenin protects against isoniazid- and rifampicin-induced apoptosis in hepatic injury. World J. Gastroenterol. 22 (44), 9775–9783. https://doi.org/10.3748/wjg.v22.i44.9775.
Wang, Y.M., Chai, S.C., Brewer, C.T., Chen, T., 2014. Pregnane X receptor and drug-induced liver injury. Expet Opin. Drug Metabol. Toxicol. 10 (11), 1521–1532. https://doi.org/10.1517/17425255.2014.963555.
Williams, G.M., 2001. Mechanisms of chemical carcinogenesis and application to human cancer risk assessment. Toxicology 166 (1–2), 3–10.
Willson, T.M., Kliewer, S.A., 2002. PXR, CAR and drug metabolism. Nat. Rev. Drug Discov. 1 (4), 259–266. https://doi.org/10.1038/nrd753.
Yang, K., Kock, K., Sedykh, A., Tropsha, A., Brouwer, K.L., 2013. An updated review on drug-induced cholestasis: mechanisms and investigation of physicochemical properties and pharmacokinetic parameters. J. Pharmacol. Sci. 102 (9), 3037–3057. https://doi.org/10.1002/jps.23584.
Yoon, E., Babar, A., Choudhary, M., Kutner, M., Pyrsopoulos, N., 2016. Acetaminophen-induced hepatotoxicity: a comprehensive update. J Clin Transl Hepatol 4 (2), 131–142. https://doi.org/10.14218/JCTH.2015.00052.
Zhou, J., Zhai, Y., Mu, Y., et al., 2006. A novel pregnane X receptor-mediated and sterol regulatory element-binding protein-independent lipogenic pathway. J. Biol. Chem. 281 (21), 15013–15020. https://doi.org/10.1074/jbc.M511116200.